Electrodialytic treatment of secondary mining resources for raw materials extraction: Reactor design assessment

J. Almeida*[1], C. Magro[1], A. R. Rosário[1], E. P. Mateus[1] and A. B. Ribeiro*[1]

[1]CENSE – Center for Environmental and Sustainability Research, Department of Sciences and Environmental Engineering, NOVA School of Science and Technology, NOVA University Lisbon, 2829-516 Caparica, Portugal

*Corresponding authors.

E-mail addresses: js.almeida@campus.fct.unl.pt (J. Almeida); abr@fct.unl.pt (A.B. Ribeiro)

Highlights

- Electrodialytic extraction of arsenic, copper, tin and tungsten was assessed.
- Electrodialytic 2 and 3-compartment reactors were studied applying 50 or 100 mA.
- Effluent and NaCl were tested as enhancements on electrodialytic setups.
- The highest extractions occurred in a 3-compartment reactor with NaCl as enhancement.
- Copper, tin and tungsten extraction were 10−13% while for arsenic was 63%,

Abstract

The sustainability of mining activities is compromised due to the high amounts of mining residues generated that have to be disposed of, often in open dams, that may cause environmental deterioration, e.g. release of toxic elements to water supplies. These residues are, however, secondary resources of raw materials. In the case of Panasqueira mine, they even are a source of tungsten, considered a critical raw material. The present work aims to assess the electrodialytic process efficiency for raw materials extraction from Panasqueira mine residues. Experiments were performed with 2 and 3-compartment electrodialytic reactors, applying current intensities between 50 and 100 mA, from 4 to 14 days, and sample suspensions

enhanced with NaCl or effluent. Additionally, control experiments with no current application were carried out. The results showed that a 3-compartment reactor operating at 100 mA, with NaCl as supporting electrolyte, presented the highest extraction of copper (13%), tin (10%), tungsten (13%) and arsenic (63%).

Keywords: Mining residues, Electrodialytic treatment, Tungsten, Copper, Tin, Arsenic

1 Introduction

The market of raw materials has increased the demand over the last few years across the globe (Mancini et al., 2019). Raw materials, constituents or substances used in goods primary production or manufacturing, are essential for human well-being and can influence the sustainable development. Their production, consumption and end-of-life is causing numerous environmental and social negative impacts (Mancini et al., 2019; Schreck and Wagner, 2017).

To tackle reliable and undistorted access to raw materials and improve growth and competitiveness of the EU economy, the European Commission (EC) launched the Raw Materials Initiative in 2008 (EC, 2008). In this context, EC has been presenting and updating the critical raw materials list, based on current raw materials economic relevance and supply risk (EC, 2017). Europe's transition towards a circular economy has been stimulated through secondary resources recovery, contributing to 'close the loop' of product life cycles (EC, 2020).

Mining residues are often a slurry of fine materials as a result of metals separation from mined ores. Their large production generates landscape and serious environmental problems. Besides the mining operation itself, the most significant impacts are waste rock dumps and residues disposal (Almeida et al., 2020a).

Panasqueira mine (Centro Region, Portugal) has been working for more than a century, being on the top list of the largest tin (Sn)-tungsten (W) deposits in Europe (Candeias et al., 2014a). The well-known tungsten trioxide (WO_3) production from wolframite, with grades up to 75%, is one of the best quality W products worldwide (Yang et al., 2016). Additionally, Panasqueira mine has a secondary production of copper (Cu) from chalcopyrite and Sn from cassiterite (Yang et al., 2016).

Panasqueira area is occupied with piles of mining residues and mud dams, nearby small villages and Zêzere river (Coelho et al., 2014). The presence of sulfides, such as arsenopyrite, presents severe risks for the surrounding ecosystem, namely for water resources. Secondary products are discharged to dams with 30% of arsenic (As) contents, that are prone to be released into various environmental compartments (Candeias et al., 2014b). According to Portuguese legislation (Diário da República, 2017), As concentration in water for public consumption must be below 10 µg As/L. Due to its characteristics, mining activities, and consequently their residues, have been one of the focus for the sustainable development goals (Mancini et al., 2019).

Research and technology have empowered the reuse of mining secondary resources, particularly focusing in construction products (Almeida et al., 2020a). However, the pH conditions may affect the leachability of As from a cement matrix (Randall, 2012). To assure safety requirements and to tackle primary resources over exploitation, versatile technologies are needed for harmful substances and raw materials extraction, namely critical metals.

The electrodialytic treatment (ED) is used to remove inorganic and organic contaminants from liquid or solid matrices (Ribeiro and Rodríguez-Maroto, 2006). When a low-level direct current is applied between pairs of electrodes, the movement of charged contaminants is promoted (Guedes et al., 2014). Three main mechanisms are responsible for contaminants´ transport:

electromigration, electroosmosis and electrophoresis. Ion exchange membranes are used to separate the contaminated matrix and to control the electrolyte conditions. The water electrolysis at inert electrodes generates an acidic media at the anode (H^+) and an alkaline media at the cathode (OH^-) (Ribeiro and Rodríguez-Maroto, 2006).

The ED process has long been applied to mining resources aiming the extraction of materials (Hansen et al., 2007), namely from sulfidic reserves (Zhang et al., 2019). Furthermore, strong acids and acidic salts such as H_2SO_4, HNO_3 and NH_4Cl, have been used to assist the process and improve the extraction ratios (Hansen et al., 2007; Ortiz-Soto et al., 2019). The implementation of green chemistry principles would promote the sustainable growth of ED technologies (Chen et al., 2020) for this application. In this sense, due to their low volatility and toxicity, natural deep eutectic solvents (DES) were applied on the extraction of metals and alloys, as As and W (Almeida et al., 2020c). Additionally, the reuse of available liquid secondary resources, as effluent from wastewater treatment plants, could also be an alternative for ED enhancing purposes. This would decrease effluent discharges and tap water consumption needed for sample suspensions preparation (Almeida et al., 2020b).

The present work aimed to assess the feasibility of Cu, Sn, W and As extraction from Panasqueira mining residues through the electrodialytic process. Several reactor setups and experimental conditions were tested to understand raw materials behavior and optimize a bottom-line treatment strategy.

2 Experimental

2.1 Materials

Mining residues mud was directly sampled from the sludge circuit output of Panasqueira mine (Covilhã, Portugal, 40°10′11″N, 7°45′24″W). Typically, this mud contains fines with particle sizes lower than 2 mm diameter (Castro-Gomes et al., 2011). The annual production of W at

Panasqueira mine is estimated in around 90,000 t with concentrated grades of approximately 75% WO_3 (Franco et al., 2014). Panasqueira samples were dried at 20 ºC for 48 h in a fume hood, before starting the experiments. Effluent was collected from the secondary clarifier (May 2019) of a wastewater treatment plant located in Lisbon (Portugal) and all the experiments were performed with samples from the same batch.

2.2 Elements extraction analysis

The concentration of As, Cu, Sn and W in the sample was determined after a pre-treatment in accordance with EPA3051A (USEPA, 2007): 0.5 g of dry sample, 9 mL of HNO_3 (65%) and 3 mL of HCl (38%) were placed in a vessel and extracted in a Microwave (Milestone Ethos, Bergamo, Italy). The microwave program was set to reach 175 ºC in 15 min, and to keep the temperature for the next 15 min. After, the samples were collected and filtered through a 1.2 µm MFV3 glassmicrofibre filters (Filter lab, Barcelona, Spain) and stored until analysis. Liquid samples (electrolyte and suspensions liquid phase) were also filtered through a 1.2 µm MFV3 glassmicrofibre filters (Filter lab, Barcelona, Spain) and stored until analysis. As, Cu, Sn and W contents were measured in an Inductively Coupled Plasma – Atomic Emission Spectrometer (ICP–AES), Varian 720-ES. For Cl^- and SO_4^{2-} quantification, 5 g of mining residues were mixed with 25 mL deionized H_2O and placed in a shaking table for 24 h, at room temperature. The samples were prior filtered by vacuum, using 1.2 µm MFV3 glassmicrofibre filters (Filter lab, Barcelona, Spain) and further analyzed by ion chromatography (DIONEX ICS-3000 equipment, Waltham, USA), equipped with conductivity detector and a Thermo Ionpac AS9-HC AG9HC column (250 × 4 mm). The eluent used was Na_2CO_3 (8 mM) at a flow rate of 1 mL/min. The sample injection volume was 10 µL at 25 ºC.

2.3 pH desorption tests

To determine the pH influence in As, Cu, Sn and W desorption, 2.5 g of mining residues were suspended in 12.5 mL of different concentrations of HNO_3 and NaOH, as well as in deionized H_2O, in order to have solutions with pH between 1 and 14. The suspensions were placed in a shaking table for one week, at room temperature. At the end, pH was measured with an EDGE, electrode meter (HANNA Instruments, Rhode Island, USA). The suspensions were filtered by vacuum using 1.2 μm MFV3 glassmicrofibre filters (Filter lab, Barcelona, Spain) and As, Cu, Sn and W concentrations were determined by ICP-AES.

2.4 Electrodialytic laboratory reactor

The experiments were carried out in a 2-compartment (2C) and 3-compartment (3C) ED reactor (Fig. 1). The reactors had an internal diameter of 8 cm and were separated by commercial anion and/or cation exchange membranes, from Ionics (AR204SZRA and CR67, MKIII, Blank, respectively). The compartment where the mining residues were placed had a length of 10 cm in the 2C configuration, and of 5 cm in the 3C setup. The electrolyte (anolyte or catholyte) compartment had a length of 5 cm. A pair of electrodes were placed in the reactor according to its design. The platinized titanium, with a 0.3 cm diameter and a length of 5 cm (Bergsøe Anti Corrosion A/S, Herfoelge, Denmark), were selected for the system due to its performance reported in other ED studies (Ferreira et al., 2018; Magro et al., 2020). A power supply (Hewlett Packard E3612A, Palo Alto, USA) was used to maintain a constant direct current and voltage drop was also monitored (Kiotto KT 1000H multimeter). The electrolyte, 0.01 M $NaNO_3$ (PanReac Appli Chem ITW Reagents, Germany), was recirculated by means of a peristaltic pump (Watson-Marlow 503 U/R, Watson-Marlow Pumps Group, Falmouth, Cornwall, UK), with one head and two extensions.

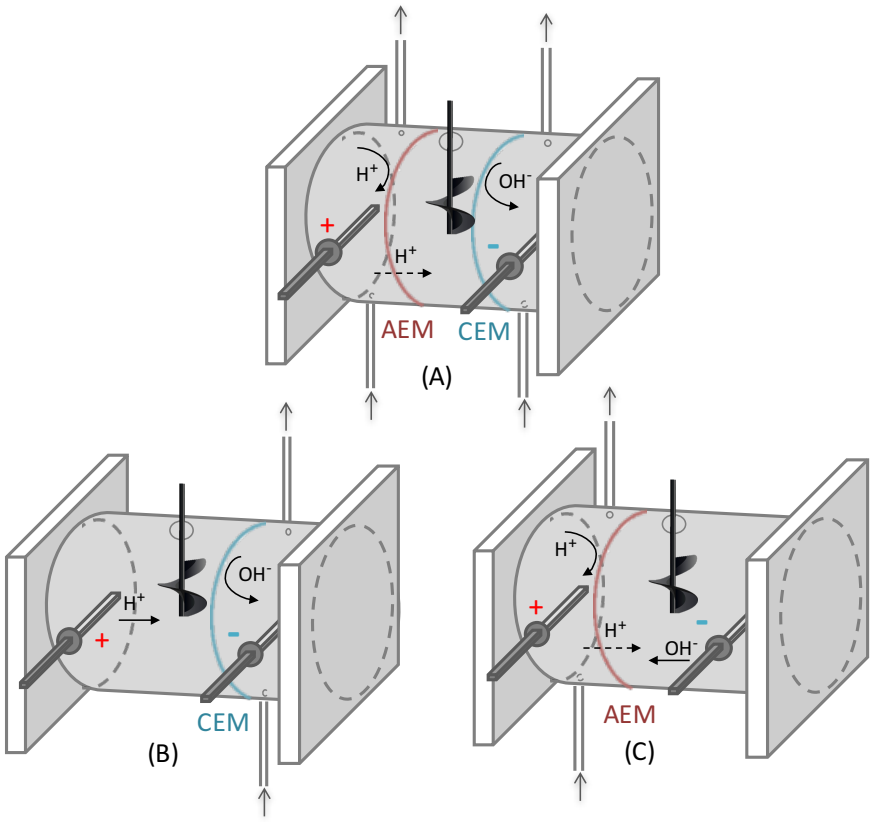

Fig 1. Schematic design of the electrodialytic laboratory tested reactors: (A) 3-compartments, 3C; (B) 2C with CEM - cation exchange membrane, and (C) 2C with AEM - anion exchange membrane.

2.5 Electrodialytic experimental conditions

In total, ten experiments were performed with constant and sequential current intensities, different reactor setups, operation times and enhancing agents (Table 1). E1-E3 experiments were performed under regular ED conditions (no enhancement agent), BW, EF1-EF3 experiments were performed adding NaCl or effluent to the sample compartment as enhancing agents, and C1-C3 were conducted with no current applied, working as control tests.

In the 2C reactors, the sample compartment was filled with 39 g of mining residues and 350 mL of deionized H_2O or effluent (EF), while in the 3C setup 22.2 g of sample were added to 200 mL of deionized H_2O, both with a Liquid/Solid (L/S) ratio of 9. For the experiment with 3C configuration, in order to ensure enough conductivity to test this design, a brine solution

157 was created by adding 11 g of NaCl to the deionized H_2O present in the sample suspension
158 compartment (BW experiment).

159 The electrolyte was recirculated using a flow rate of 3 mL/min in the electrolytes compartments.
160 To guarantee the suspension of the mining residues, a magnetic stirrer was used in the sample
161 compartment. All the experiments were performed in a fume hood at room temperature.

162 *Table 1. Electrodialytic experimental conditions*

Experiment	Setup	Membrane	Current (mA)	Sample compartment	Running days
ED experiments (n=2)					
E1	2C	CEM	100	Anode	14
E2	2C	AEM	100	Cathode	14
E3	2C	AEM	50	Cathode	8
Enhanced ED experiments (BW n=2; EF n=1)					
BW	3C	AEM and CEM	100	Central	5
EF1[b]	2C	AEM	50	Cathode	4
EF2[b]	2C	CEM	50	Anode	4
EF3[b]	2C	AEM	65-55-45-35[a]	Cathode	4
Control experiments with no current (n=2)					
C1	2C	AEM	0	Cathode	10
C2	2C	CEM	0	Anode	10
C3	3C	AEM and CEM	0	Central	10

163 BW – Brine water; EF – Effluent; AEM – Anion exchange membrane; CEM – Cation exchange membrane.
164 [a]Sequential decreasing current intensity, n – number of experiments performed, [b]effluent was placed in the sample
165 compartment.

166

167

2.6 Statistical analysis

Statistically significant differences among samples for 95% level of significance were evaluated through ANOVA tests using GraphPad Prism software (version 8). Statistical differences were analyzed for pH and conductivity variations in the reactor compartments, and for elements extraction considering: (1) same element, different experiments, and (2) same experiment, different elements. The notation selected to present statistically significant differences among the results obtained was lower case letter versus same capital letter. Thus, data with lower case letter is statistically significant different from the data with the same capital letter, with 95% confidence interval.

3 Results and discussion

3.1 Initial characterization

Table 2 presents the initial composition of mining residues by ICP-AES method. Regarding the target compounds, As presented the highest concentration (3743 ± 471 mg/kg), comparing to the contents of Cu (1790 ± 202 mg/kg), Sn (75 ± 8 mg/kg) and W (488 ± 88 mg/kg) in the sample. The presence of salts and other elements, namely Fe (7250 ± 318 mg/kg) and SO_4^{2-} (217 ± 5 mg/kg), may influence ions mobility due to uncharged complexes generation, affecting elements extraction by ED (Almeida et al., 2020b).

Table 2. Composition of mining residues.

Parameter	mg/kg
ICP-AES analysis	
As	3743.2 ± 471.0^{a}
Ca	$97.3 \pm 44.8^{A,b}$
Cu	$1790.3 \pm 202.3^{A,B,c}$
Fe	$7250.2 \pm 318.4^{A,B,C,d}$
P	$46.6 \pm 12.7^{A,C,D}$

Parameter	mg/kg
Sn	$75.11 \pm 8.6^{A,C,D}$
W	$487.8 \pm 87.5^{A,C,D}$
IC analysis	
Cl^-	$5.0 \pm 2.3^{A,C,D}$
SO_4^{2-}	$217.0 \pm 4.6^{A,C,D}$

ICP-AES, Inductively Coupled Plasma - Atomic Emission Spectrometer.

IC - Ion Chromatography.

Statistical analysis was carried out at $p < 0.05$ (95% confidence interval). Data with lower case letters are statistically significantly different to data with the same capital letter.

3.2 Electrodialytic experiments

During the ED treatment, pH fluctuations occurred due to electrode reactions (described later in Eqs. 1 and 2). Accordingly, desorption tests were performed before the remediation process to understand As, Cu, Sn and W concentration in the aqueous phase as function of pH (Fig. 2).

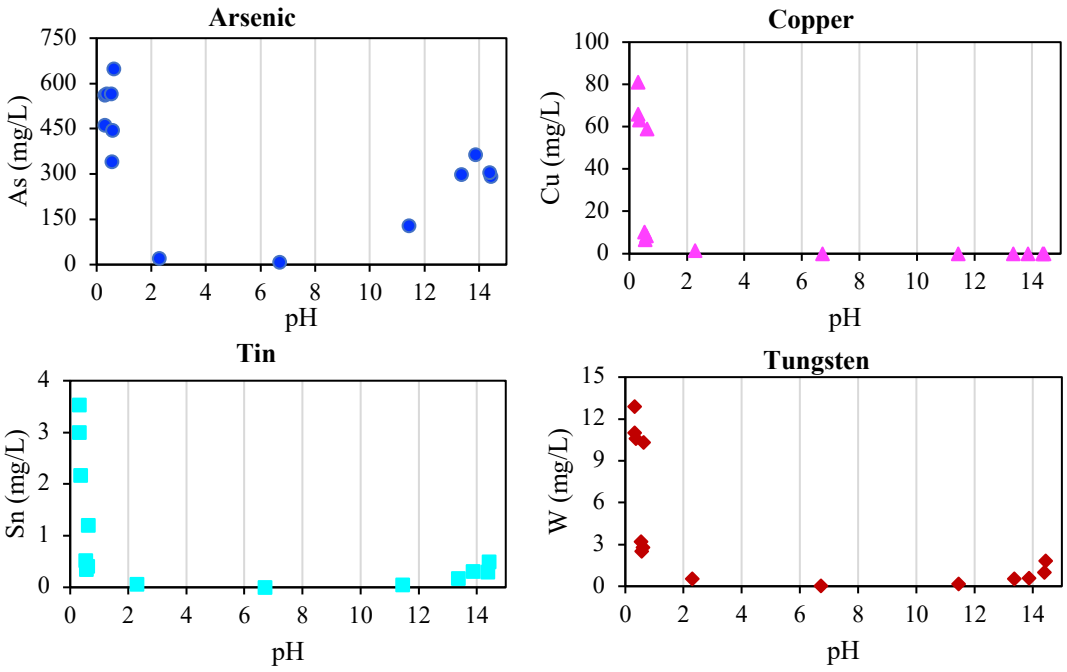

Fig 2. Arsenic, copper, tin and tungsten pH desorption at different concentrations of HNO_3 and NaOH solutions with pH between 1 and 14.

The solubility of compounds, namely oxides, hydroxides, carbonates or mineral forms, is highly dependent on the media pH. Also, cationic/anionic constituents are related to solid residues through adsorption/desorption on mineral or organic surfaces with a pH-dependent charge. Dissolution and sorption processes provide a pH-dependent leaching trend where the release of cations increases in low pH media and the release of anions increases towards high pH solutions (Król et al., 2020).

Generally, elements desorption from mining residues were higher at pH values below 2 (Fig. 2) due to the chemical speciation of the studied elements, where the release of cationic species was more pronounced. Only As showed a second desorption peak at pH above 11. At high pH, $HAsO_4^{2-}$ is the dominant As species, followed by AsO_4^{3-} considering an oxidizing media. These anions can react with Ca^{2+} to form amorphous or crystalline arsenate (Vempati et al., 1995). This means that during the ED process the sample should be theoretically placed at the anode compartment, where an acidic pH (below 2) is promoted and, as a consequence, higher desorption rates are expected. Considering the ED system, it is foreseen that the most common forms of As, Cu, Sn and W, in extreme acidic conditions and with soluble forms at pH below 2 are, respectively, H_3AsO_4/H_3AsO_3 (Chen et al., 2014), $Cu^{2+}/Cu(OH)^{+}$ (Cuppett et al., 2006), $Sn^{2+}/Sn(OH)^{3+}$ (Dulnee and Scheinost, 2015) and WO_3 (Cao and Guo, 2019). Nevertheless, the mobility of these elements during ED experiments may be limited due to eventual complexation with other substances present in the media (Almeida et al., 2020b).

In a first stage, the ED process was applied considering 2C and 3C reactors at 50 and/or 100 mA. The pH behavior of the sample compartment during the treatment is presented in Fig. 3a.

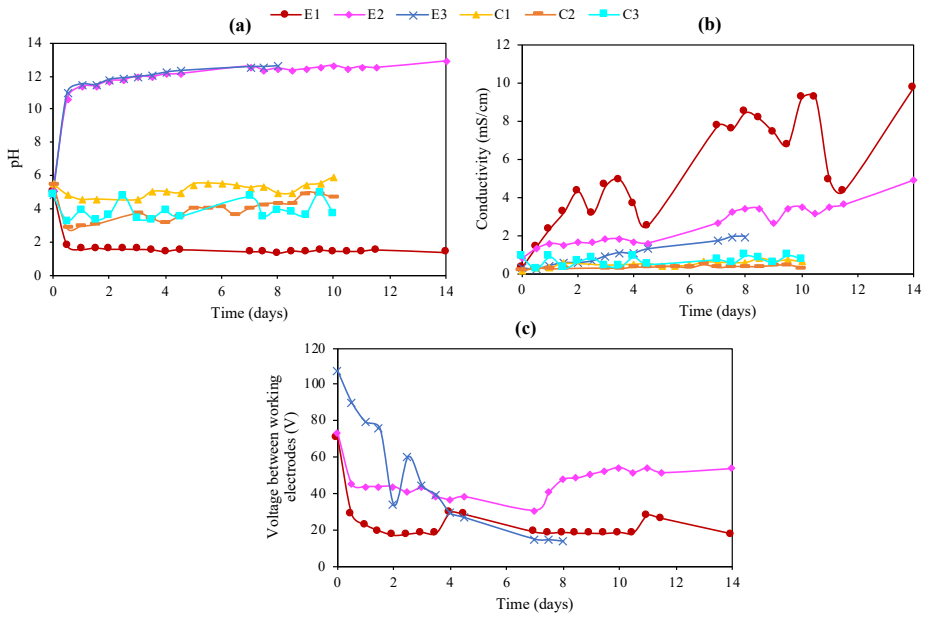

The values were collected daily, except on weekends and national holidays.

Fig 3. Mining residues: (a) pH, (b) conductivity and (c) voltage between working electrodes during the electrodialytic experiments. E1-CEM,100 mA; E2-AEM, 100 mA; E3-AEM, 50 mA; C1-control AEM; C2-control CEM; C3-control AEM and CEM.

Generally, after the ED process, sample pH decreased when mining residues were placed in the anode compartment (Fig. 1b), while the opposite was verified when the matrix was at the cathode compartment (Fig. 1c). Sample pH increased in E2 and E3 tests and decreased in E1 test. This was expected due to water electrolysis phenomena occurrence at the electrode compartments. Herein, H^+ is generated at the anode (Eq. 1) while OH^- is formed at the cathode end (Eq. 2), promoting an acidic and alkaline pH media, respectively. Also, the presence of chloride in the ED system may lead to the formation of active chlorine, which is an oxidant agent (Eq. 3).

$$H_2O\ (l) \longrightarrow \frac{1}{2}O_2\ (g) + 2H^+ + 2e^- \quad (1)$$

$$H_2O\ (l) + e^- \longrightarrow \frac{1}{2}H_2\ (g) + OH^- \quad (2)$$

$$Cl_2\ (g) + 2e^- \longrightarrow 2Cl^- \quad (3)$$

As the pH in the residue suspension decreases, a higher dissolution of the residue is expected (Fig. 2). Fig. 3 (b) and (c) also shows the conductivity behavior and the voltage variation on the sample compartment during the experiments, respectively.

Conductivity in the media has to be assured to promote current passage and electrochemically-induced extraction of substances. Typically, mining residues are characterized by low conductivity values, with an average of 0.3 mS/cm (Almeida et al., 2020c; Almeida et al., 2020b; Magro et al., 2019). The initial electrical conductivity of the suspension was in average approximately 1 mS/cm (Fig. 3). When a 2C reactor design was tested (E1, E2 and E3), the conductivity of the sample compartment tended to increase (Fig. 3b), due to the generation of free ions in the media (Eqs. 1 and 2), which was advantageous for current passage and, consequently, for the ED process performance. This increase was more pronounced at the end of E1 (9.8 mS/cm) and E2 (4.9 mS/cm), where 100 mA were applied. However, there are oscillations in the conductivity, namely in E1. This may be explained by CEM properties, since sulphonation is required to maintain good conductivity, ion exchange capacity and permselectivity on the system. A high degree of sulphonation may have caused instability (Shukla and Shahi, 2019).

A voltage decrease tendency was verified (Fig. 3c), due to the decrease of the internal resistance in the reactor along the experiments, based on Ohm law (Eq. 4):

$$I = \frac{V}{R} \qquad (4)$$

where I is the current intensity (in amperes), V is the voltage (in volts) and R the resistance (in ohms) applied.

Moreover, when the current was applied, the pH at the anolyte compartment decreased to around 2, while the pH at the catholyte compartment increased until approximately 10 (Table S1, in appendix A). In all experimental setups, conductivity increased at the end of the

experiments, from approximately 1 to 4−6 mS/cm. This was predictable due to the increment of free ions, corroborating the generation of ions by the electrodes and the electromigration of substances from the sample to the electrolyte compartments.

Furthermore, when mining residues were placed in the central compartment (3C reactor case, Fig. 1a), the current passage was not facilitated due to the extremely low conductivity of the sample, being unfeasible to operate the process according to the time set for the experiments, without the addition of adjuvants. Electrokinetic effects promote non-homogenous slipping flows over charged surfaces, which may impact hydrodynamics of tight porous materials, as mining residues (Karaca et al., 2017). Regarding the transport of ionic solutions, both hydrodynamic and electrokinetic transport are expected. However, the transport due to electric fields (e.g. electroosmosis) is more prominent in tight pores where electrical diffuse layer is not negligible (Godinez-Brizuela and Niasar, 2020).

In fact, the ED 3C reactor could not perform properly without adding enhancing agents, to assure enough conductivity in the media and avoid operation problems, such as pressure fluctuations inside the reactor during the operation time. Considering this limitation, mining residues were treated in a 3C reactor design adding brine water (BW), and in 2C reactor designs using effluent (EF) as enhancing agents (Table 1). Whereas NaCl was added to the sample compartment only to assure enough conductivity, effluent was tested as an eco-friendlier alternative, comparing to water, in both 3C and 2C reactor designs. Additionally, the application of decreasing current intensities was tested in solid matrices (Guedes et al., 2016). Thus, a sequential decreasing current intensity was applied to an effluent experiment to test their feasibility on ED experiments, aiming to improve the process efficiency and the overall stability of the ED system.

Table 3 presents pH, conductivity and voltage behavior on enhanced ED experiments with EF and BW.

Table 3. Initial and final pH, conductivity and voltage values in the reactor's compartments, on enhanced ED experiments.

Experiment	Compartment	pH		Conductivity (mS/cm)		Voltage between working electrodes (V)	
		Initial	**Final**	**Initial**	**Final**	**Initial**	**Final**
BW (3C)	Cathode	6.8 ± 0.2	3.5 ± 0.5	0.7 ± 0.1^{b}	6.3 ± 1.6^{d}	29.2 ± 9.1	16.2 ± 1.4
	Central (sample)	5.3 ± 0.7	4.5 ± 1.0^{a}	12.6 ± 1.6^{B,c}	3.8 ± 1.2^{e}		
	Anode	6.8 ± 0.2	1.5 ± 0.1^{A}	0.7 ± 0.1^{C}	13.5 ± 1.6^{D,E}		
EF1 (2C)	Cathode (sample)	7.5	12.4	1.6	2.2	20.5	14.5
	Anode	8.0	1.9	1.1	5.0		
EF2 (2C)	Cathode	7.6	12.4	0.7	1.9	22.7	8.4
	Anode (sample)	4.82	2.2	0.8	1.5		
EF3 (2C)	Cathode (sample)	7.6	12.7	0.7	3.2	32.3	11.8
	Anode	4.8	2.7	0.8	1.6		

Statistical analysis was carried out at $p < 0.05$ (95% confidence interval). Data with lower case letters are statistically significantly different to data with the same capital letter.

The same pH, conductivity and voltage trends verified on Fig. 3 were observed in enhanced experiments. The sample pH decreased to around 2 when mining residues were placed at the anode, and increased to approximately 12, when the sample was at the cathode compartment. Concerning the BW experiment (performed in the 3C reactor), the pH at the central compartment decreased from 5.3 to 4.5, once the anion exchange membrane has limited

permselectivity (Ribeiro and Rodríguez-Maroto, 2006). Only protons (H^+) are able to cross this membrane, promoting the decrease of the pH in the central compartment, during the experiment. Conductivity dropped about 70% in the central compartment at the end of experiment, due to the electromigration of charged species towards the electrolyte compartments. Thus, a conductivity increase was verified in the cathode (6.3 ± 1.6 mS/cm) and anode (13.5 ± 1.6 mS/cm) compartments, where the second was more pronounced (Table 3).

On experiments performed with 2C reactors, using effluent as an enhancing agent, the pH at the anode compartment decreased to around 2, while the pH at the cathode compartment increased until approximately 12. The conductivity at the end of the experiments in the sample compartment increased in all experiments. The experimental behavior was similar to E1, E2 and E3 experiments (Fig. 3), corroborating that water replacement by effluent to perform the liquid suspension did not significantly affect the ED system balance.

Electrochemical reactions that occur at the anode and cathode (oxidation and reduction) may contribute to the increase of conductivity in the media. The removal process may cause the presence of more ions in solution (free ions), and consequently higher conductivity at the end of the experiments. As expected in all tested cases, the voltage values decreased as electrical conductivity increased, which is in line with Ohm's law. BW voltage decrease from around 29 to 16 V; EF1 from 21 to 15 V; EF2 from 23 to 8 V and EF3 from 32 to 12 V (Table 3).

3.3 Elements extraction

After the ED process, As, Cu, Sn and W final distribution in the reactor compartments was assessed. Fig. 4 presents the amounts of each studied element detected at the anode (anolyte), cathode (catholyte) and sample (solid sample and liquid phase) compartments, for all experiments performed.

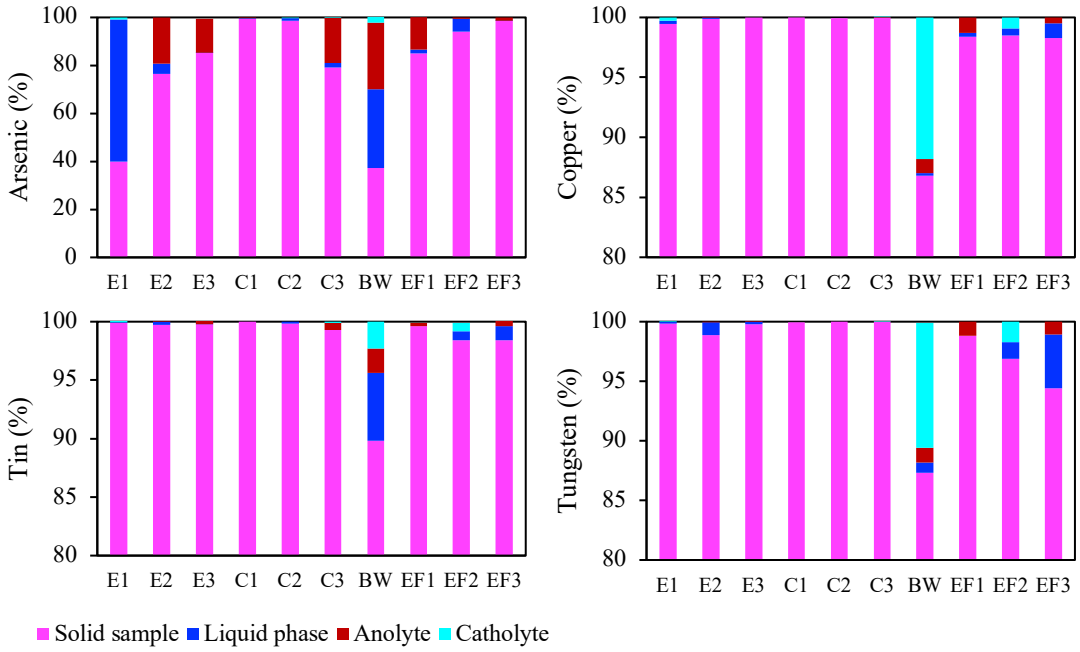

316

317 *Fig 4. Arsenic, copper, tin and tungsten distribution in the ED reactor after the ED experiments. E1-CEM, 100*
318 *mA; E2-AEM, 100 mA; E3-AEM, 50 mA; C1-control AEM; C2-control CEM; C3-control AEM-CEM; BW-AEM-*
319 *CEM, NaCl, 100 mA; EF1-AEM, 50 mA; EF2-CEM, 50 mA; EF3-AEM, 65-55-45-35 mA (*sequential current
320 intensity).

321

322 Generally, after the ED experiments (E1, E2 and E3), As demonstrated the highest mobility
323 since As was detected in the anolyte on experiments E2 (19%) and E3 (14%). Thus,
324 predominant As extraction was observed towards the anode, where the rising current intensity
325 promoted its speciation. Also, 60% of As was solubilized in the liquid phase on E1. Only trace
326 amounts of Cu (0.3%), Sn (0.3%) and W (0.1%) were detected in the solid sample at E1. Copper
327 was detected at the cathode compartment and in the liquid phase in E1, while Sn and W where
328 mainly detected in E1 at the catholyte (Sn = 0.3%; W = 0.01%) and in E2 in the liquid phase of
329 the sample suspension (Sn = 0.02 %; W = 1.1 %).

330 Contrarily, enhanced experiments (BW, EF1, EF2 and EF3), demonstrated an increase on
331 elements extraction. BW showed the highest electromigration rates, since elements were
332 detected in the anode and in the cathode compartments. Arsenic was detected in the anolyte

333 (28%), while Cu (12%) and W (11%) were mainly detected at the anode end. Tin was detected
334 in both electrolyte compartments in the same proportion (2%). Regarding effluent experiments,
335 advantages namely for Cu, Sn and W extraction were observed, when compared to E1, E2 and
336 E3 experiments. Copper, Sn and W were detected in higher percentages at the anode on EF1
337 and at the cathode on EF2. The solubilization of Cu (1%), Sn (1%) and W (5%) was obtained
338 when the ED experiment was performed with a combination between effluent and the
339 application of a sequential decreasing current intensity (EF3), that may improve ED efficiency
340 and stability. Thus, the combination of the three tested setups could present advantages for the
341 extraction of Cu, Sn and W.

342 The possible complexation of metals with substances present in the media may have hindered
343 the extraction and electromigration rates towards the electrolyte's compartments. At lower pH,
344 As can form insoluble complexes with Fe oxides as $AsFeO_4$, since high levels of Fe are present
345 in the sample (7250 ± 318 mg/kg, Table 2). Thus, arsenate species may react in an easier way
346 with ferrous ions, inhibiting at the same time Fe reaction with other species, also present in
347 solution (Guan et al., 2011). This type of As, associated to insoluble complexes, is immobile.
348 However, in the reduction state, arsenite is predominant and the complexes formed are mobile
349 (Yang et al., 2015). The presence of Ca (97 ± 45 mg/kg) in the sample may promote the
350 generation of $Ca_3(AsO_4)_2$ as well (Mahapatra et al., 1984). Copper complexation may also occur
351 in presence of As ($Cu(OH)AsO_4$) (De Pedro et al., 2011), Fe ($CuFe_2O_4$) (Satheeshkumar et al.,
352 2019) or SO_4^{2-} ($CuSO_4$) (Xi et al., 2019), limiting Cu extraction. Additionally, Sn complexes
353 may also be formed in the presence of Cu, as Cu_6Sn_5 or Cu_3Sn (Liu et al., 2016).

354 The W most common form is WO_3, which is present in solution at pH below 2. In addition,
355 SO_4^{2-} presence (217 ± 5 mg/kg, Table 2) may promote the formation of $WO_2(SO_4)_3^{4-}$. These
356 species also blocks oxygen reduction reaction, which is already low in cationic dissolution in

357 electrochemical processes (Lassner and Schubert, 1999). $CaWO_4$ may also be formed in the
358 present conditions (Yekta et al., 2016), complicating W extraction.

359 In lower proportions, due to the Cl^- presence in the initial sample (5 ± 2 mg/kg, Table 2),
360 $AsCl_3$ (Cazzoli et al., 1978), $[CuCl_2]^-$ (Cotton et al., 1974), $SnCl_3^-$ or $SnCl_4^{2-}$ (Sherman et al.,
361 2000) and $[W_2Cl_9]^{3-}$ (Rollinson, 1973) may also be formed. However, when NaCl was added
362 to the sample suspension in BW (11 g) and also during effluent experiments, which is also reach
363 in Cl^- (193 mg/L, Table S2 in appendix A) (Magro et al., 2020), the increase in Cl^- content
364 may have potentiated the formation of the species mentioned, promoting at the same time their
365 extraction.

366 The summary of the extraction of the studied elements from the original matrix is presented in
367 Table 4.

368

369

370

371

372

373

374

375

376

377

Table 4. Arsenic, copper, tin and tungsten extraction from mining residues after ED experiments.

Experiment	Extraction (%)			
	Arsenic	**Copper**	**Tin**	**Tungsten**
E1	60.1 ± 24.1^{a}	0.6 ± 0.5^{A}	0.3 ± 0.1^{A}	0.1 ± 0.1^{A}
E2	$23.4 \pm 3.9^{A,b}$	0.1 ± 0.1	0.3 ± 0.2	1.1 ± 0.3
E3	$14.3 \pm 0.5^{A,c}$	n.d	0.4 ± 0.1	0.4 ± 0.1
BW	$63.2 \pm 28.3^{B,C,d}$	13.4 ± 1.7^{D}	10.2 ± 6.7^{D}	12.6 ± 3.6^{D}
EF1	15.1	1.6	0.4	1.2
EF2	5.8	1.5	1.6	3.1
EF3	1.5	1.7	1.6	5.6
C1	$0.5 \pm 0.2^{A,D}$	n.d	n.d	n.d
C2	$1.1 \pm 0.3^{A,D}$	n.d	0.2 ± 0.2	n.d
C3	$21.0 \pm 0.6^{A,D}$	0.1 ± 0.1	0.7 ± 0.3	n.d

n.d – not detected.

Statistical analysis was carried out at $p < 0.05$ (95% confidence interval). Data with lower case letters are statistically significantly different to data with the same capital letter.

*E1-CEM, 100 mA; E2-AEM, 100 mA; E3-AEM, 50 mA; C1-control AEM; C2-control CEM; C3-control AEM-CEM; BW-AEM-CEM, NaCl, 100 mA; EF1-AEM, 50 mA; EF2-CEM, 50 mA; EF3-AEM, 65-55-45-35 mA (*sequential decreasing current intensity).

According to Table 4, As showed the highest extraction ratios, compared to the other studied elements. A maximum of 63% of As was successfully extracted from the matrix in the BW experiment, whereas Cu, Sn and W extraction reached 13, 10 and 13%, respectively. Arsenic may have been solubilized from the solid to the liquid phase of the sample compartment due to the pH changes that lead to its speciation. The changes in As oxidation states may have

391 generated a “mobile phase” of this element, potentiating its electromigration to the
392 anolyte/catholyte compartment. Moreover, As extraction is statistically significantly different
393 (p value < 0.0001) compared to As extraction in other experiments, and to Cu, Sn and W in the
394 same experiment (E1 and BW).

395 **4 Conclusions**

396 Generally, secondary mining residues are stable matrices with low conductivity, implying
397 changes both in the ED reactor design and in the process itself. From the results obtained it was
398 observed that an ED 3C reactor might be the most suitable setup for raw materials extraction,
399 comparing to ED 2C systems. The conductivity increases by the addition of NaCl on the sample
400 compartment improved the current passage, and consequently, the species extraction (As =
401 63%; Cu = 13%, Sn = 10% and W = 13%).
402 At the studied conditions, the ED process potential for Cu, Sn and W extraction from the mining
403 residues is lower than for As, due to the poorer solubilization and migration rate of species to
404 the electrolyte compartments.
405 Arsenic was successful extracted from the initial sample during the tests performed due to its
406 conversion into mobile forms. Contrarily, raw materials ED extraction was mainly affected by
407 the presence of other compounds in solution, where the formation of complexes inhibited the
408 migration of the elements inside the reactor. However, the development of different treatment
409 stages can overcome the electromigration low rate.
410 The application of enhancements could be a key factor to improve elements extraction ratios
411 from the mining residues. Additionally, ED operation time could be optimized, promoting
412 savings in terms of labor and energy costs.
413 Summing up: The improvement of the ED performance targeting the Panasqueira mine residues
414 was achieved by adding eco-friendly enhancements as NaCl and effluent, particularly to As, as

mobile forms were obtained with the generated pH changes. For Cu, Sn and W, further adjustments have to be studied in order to increase their extraction efficiencies.

CRediT authorship contribution statement

J. Almeida: Conceptualization, Methodology, Writing - original draft, Visualization, Writing - review & editing, Software, Investigation. **C. Magro:** Conceptualization, Methodology, Writing - review & editing, Investigation. **A.R. Rosário:** Conceptualization, Methodology, Investigation. **E.P. Mateus:** Validation, Resources, Writing - review & editing. A**.B. Ribeiro:** Validation, Supervision, Writing - review & editing, Funding acquisition, Resources.

Declaration of competing interest

The authors have no affiliation with any organization with a direct or indirect financial interest in the subject matter discussed in the manuscript.

Acknowledgments

This work received funding from the European Union's Horizon 2020 research and innovation program under the Marie Skłodowska-Curie grant agreement No. 778045, and from Portuguese funds from FCT/MCTES through grant UIDB/04085/2020. J. Almeida acknowledges *Fundação para a Ciência e a Tecnologia* and EcoCoRe Doctoral program for her PhD fellowship PD/BD/135170/2017. The authors acknowledge Carla Rodrigues and Nuno Costa from REQUIMTE for the ICP and IC analysis, and Eng. Manuel Pacheco from Panasqueira mine for providing the mining residues. This research is anchored by the RESOLUTION LAB, an infrastructure at NOVA School of Science and Technology.

References

Almeida, J., Ribeiro, A.B., Silva, A.S., Faria, P., 2020a. Overview of mining residues incorporation in construction materials and barriers for full-scale application. J. Build. Eng. 29, 101215. https://doi.org/10.1016/j.jobe.2020.101215

Almeida, J., Magro, C., Mateus, E.P., Ribeiro, A.B., 2020b. Electrodialytic hydrogen production and critical raw materials recovery from secondary resources. Water 12, 1262. https://doi.org/10.3390/w12051262

Almeida, J., Craveiro, R., Faria, P., Silva, A.S., Mateus, E.P., Barreiros, S., Paiva, A., Ribeiro, A.B., 2020c. Electrodialytic removal of tungsten and arsenic from secondary mine resources — deep eutectic solvents enhancement. Sci. Total Environ. 710, 136364. https://doi.org/10.1016/j.scitotenv.2019.136364

Candeias, C., Melo, R., Ávila, P.F., Ferreira da Silva, E., Salgueiro, A.R., Teixeira, J.P., 2014a. Heavy metal pollution in mine-soil-plant system in S. Francisco de Assis - Panasqueira mine (Portugal). Appl. Geochem. 44, 12–26. https://doi.org/10.1016/j.apgeochem.2013.07.009

Candeias, C., Ávila, P.F., Silva, E.F. Da, Ferreira, A., Salgueiro, A.R., Teixeira, J.P., 2014b. Acid mine drainage from the Panasqueira mine and its influence on Zêzere river (Central Portugal). J. African Earth Sci. 99, 705–712. https://doi.org/10.1016/j.jafrearsci.2013.10.006

Cao, Y., Guo, Q., 2019. Tungsten speciation and its geochemical behavior in geothermal water: a review. E3S Web Conf. 98, 07005. https://doi.org/10.1051/e3sconf/20199807005

Castro-Gomes, J.P., Silva, A., Cano, R.P., Durán Suarez, A., 2011. Recycled materials for technical-artistic applications obtained with tungsten mine coarse wastes, in: International

463 Conference on Sustainability of Constructions - Towards a Better Built Environment.
464 Innsbruck.

465 Cazzoli, G., Forti, P., Lunelli, B., 1978. Molecular structure and harmonic force field of $AsCl_3$
466 by microwave spectroscopy. J. Mol. Spectrosc. 69, 71–78. https://doi.org/10.1016/0022-
467 2852(78)90029-2

468 Chen, M.L., Ma, L.Y., Chen, X.W., 2014. New procedures for arsenic speciation: a review.
469 Talanta 125, 78–86. https://doi.org/10.1016/j.talanta.2014.02.037

470 Chen, T.L., Kim, H., Pan, S.Y., Tseng, P.C., Lin, Y.P., Chiang, P.C., 2020. Implementation of
471 green chemistry principles in circular economy system towards sustainable development
472 goals: challenges and perspectives. Sci. Total Environ. 716, 136998.
473 https://doi.org/10.1016/j.scitotenv.2020.136998

474 Coelho, P., García-Lestón, J., Costa, S., Costa, C., Silva, S., Fuchs, D., Geisler, S., Dall'Armi,
475 V., Zoffoli, R., Bonassi, S., Pásaro, E., Laffon, B., Teixeira, J.P., 2014. Immunological
476 alterations in individuals exposed to metal(loid)s in the Panasqueira mining area, Central
477 Portugal. Sci. Total Environ. 475, 1–7. https://doi.org/10.1016/j.scitotenv.2013.12.093

478 Cotton, F.A., Frenz, B.A., Hunter, D.L., Mester, Z.C., 1974. Copper(I) and copper(II)
479 complexes of tetramethyldiphosphinedisulfide. II. Isolation and characterization of a
480 polymeric copper(II) precursor, $(Me_4P_2S_2)CuCl_2$, to the ultimate copper(I) product,
481 $[(Me_4P_2S_2)CuCl]_2$. Inorganica Chim. Acta 11, 119–122. https://doi.org/10.1016/S0020-
482 1693(00)93694-6

483 Cuppett, J., Duncan, S., Dietrich, A., 2006. Evaluation of copper speciation and water quality
484 factors that affect aqueous copper tasting response. Chem. Senses 31, 689–697.
485 https://doi.org/10.1093/chemse/bjl010

De Pedro, I., Rojo, J.M., Pizarro, J.L., Rodríguez Fernández, J., Arriortua, M.I., Rojo, T., 2011. Magnetostructural correlations in the antiferromagnetic Co_2-x $Cu_x(OH)AsO_4$ (x=0 and 0.3) phases. J. Solid State Chem. 184, 2075–2082. https://doi.org/10.1016/j.jssc.2011.05.060

Diário da República, 2017. Decreto-Lei n.º 152/2017 from December 7th, Ministério do Ambiente. Diário da República: I série, Nº 235.

Dulnee, S., Scheinost, A.C., 2015. Interfacial reaction of SnII on mackinawite (FeS). J. Contam. Hydrol. 177–178, 183–193. https://doi.org/10.1016/j.jconhyd.2015.03.012

EC, 2017. Communication from the Commission to the European Parliament, the Council, the European Economic and Social Committee and the Committee of the Regions on the 2017 list of Critical Raw Materials for the EU.

EC, 2020. Communication from the Commission to the European Parliament, the Council, the European Economic and Social Committee and the Committee of the Regions - A new Circular Economy Action Plan for a cleaner and more competitive Europe. Brussels.

EC, 2008. Communication from the Commission to the European Parliament and the Council, The raw materials initiative - meeting our critical needs for growth and jobs in Europe. Brussels.

Ferreira, A.R., Couto, N., Guedes, P., Pinto, J., Mateus, E.P., Ribeiro, A.B., 2018. Electrodialytic 2-compartment cells for emerging organic contaminants removal from effluent. J. Hazard. Mater. 358, 467–474. https://doi.org/10.1016/j.jhazmat.2018.04.066

Franco, A., Vieira, R., Bunting, R., 2014. The Panasqueira mine at a Glance, Tungsten. International Tungsten Industry Association,

508 Godinez-Brizuela, O.E., Niasar, V.J., 2020. Simultaneous pressure and electro-osmosis driven
509 flow in charged porous media: Pore-scale effects on mixing and dispersion. J. Colloid
510 Interface Sci. 561, 162–172. https://doi.org/10.1016/j.jcis.2019.11.084

511 Guan, X., Dong, H., Ma, J., Lo, I.M.C., 2011. Simultaneous removal of chromium and arsenate
512 from contaminated groundwater by ferrous sulfate: Batch uptake behavior. J. Environ.
513 Sci. 23, 372–380. https://doi.org/10.1016/S1001-0742(10)60420-2

514 Guedes, P., Couto, N., Ottosen, L.M., Ribeiro, A.B., 2014. Phosphorus recovery from sewage
515 sludge ash through an electrodialytic process. Waste Manag. 34, 886–892.
516 https://doi.org/10.1016/j.wasman.2014.02.021

517 Guedes, P., Mateus, E., Almeida, J., Ferreira, A., Couto, N., Ribeiro, A., 2016. Electrodialytic
518 treatment of sewage sludge: current intensity influence on phosphorus recovery and
519 organic contaminants removal. Chem. Eng. J. 306, 1058–1066.
520 https://doi.org/10.1016/j.cej.2016.08.040

521 Hansen, H.K., Ribeiro, A.B., Mateus, E.P., Ottosen, L.M., 2007. Diagnostic analysis of
522 electrodialysis in mine tailing materials. Electrochim. Acta 52, 3406–3411.
523 https://doi.org/10.1016/j.electacta.2006.05.066

524 Karaca, O., Cameselle, C., Reddy, K.R., 2017. Acid pond sediment and mine tailings
525 contaminated with metals: physicochemical characterization and electrokinetic
526 remediation. Environ. Earth Sci. 76, 1–12. https://doi.org/10.1007/s12665-017-6736-0

527 Król, A., Mizerna, K., Bożym, M., 2020. An assessment of pH-dependent release and mobility
528 of heavy metals from metallurgical slag. J. Hazard. Mater. 384, 121502.
529 https://doi.org/10.1016/j.jhazmat.2019.121502

530 Lassner, E., Schubert, W.-D., 1999. Important aspects of tungsten chemistry, in: Tungsten -

Properties, Chemistry, Technology of the Element, Alloys, and Chemical Compounds. Springer US, Boston, MA, pp. 61–84. https://doi.org/10.1007/978-1-4615-4907-9_2

Liu, L., Chen, Z., Liu, C., Wu, Y., An, B., 2016. Micro-mechanical and fracture characteristics of Cu_6Sn_5 and Cu_3Sn intermetallic compounds under micro-cantilever bending. Intermetallics 76, 10–17. https://doi.org/10.1016/j.intermet.2016.06.004

Magro, C., Almeida, J., Paz-Garcia, J.M., Mateus, E.P., Ribeiro, A.B., 2019. Exploring hydrogen production for self-energy generation in electroremediation: a proof of concept. Appl. Energy 255, 113839. https://doi.org/https://doi.org/10.1016/j.apenergy.2019.113839

Magro, C., Mateus, E.P., Paz-Garcia, J.M., Ribeiro, A.B., 2020. Emerging organic contaminants in wastewater: understanding electrochemical reactors for triclosan and its by-products degradation. Chemosphere 247, 125758. https://doi.org/10.1016/j.chemosphere.2019.125758

Mahapatra, P.P., Mahapatra, L.M., Nanda, C.N., 1984. Dissolution of $Ca_3(AsO_4)_2 \cdot 2H_2O$ in the system CaOAs2O5H2O at 35, 40, 45 and 50°C and the related thermodynamic data. Thermochim. Acta 76, 301–309. https://doi.org/10.1016/0040-6031(84)87027-6

Mancini, L., Vidal-Legaz, B., Vizzarri, M., Wittmer, D., Grassi, G., Pennington, D.W., 2019. Mapping the role of raw materials in sustainable development goals, in: Sustainable Development Goals. A Preliminary Analysis of Links, Monitoring Indicators, and Related Policy Initiatives. Publications Office of the European Union, Luxembourg, p. JRC112892. https://doi.org/10.2760/026725

Ortiz-Soto, R., Leal, D., Gutierrez, C., Aracena, A., Rojo, A., Hansen, H.K., 2019. Electrokinetic remediation of manganese and zinc in copper mine tailings. J. Hazard.

554 Mater. 365, 905–911. https://doi.org/10.1016/j.jhazmat.2018.11.048

555 Randall, P.M., 2012. Arsenic encapsulation using Portland cement with ferrous sulfate/lime
556 and Terra-BondTM technologies - microcharacterization and leaching studies. Sci. Total
557 Environ. 420, 300–312. https://doi.org/10.1016/j.scitotenv.2011.12.066

558 Ribeiro, A.B., Rodríguez-Maroto, J.M., 2006. Trace elements in the environment:
559 biogeochemistry, biotechnology, and bioremediation, in: Prasad, M.N.V., Sajwan, K.S.,
560 Naidu, R. (Eds.). CRC Press, Florida, USA, pp. 341–368.

561 Rollinson, C.L., 1973. Tungsten compounds, in: The Chemistry of Chromium, Molybdenum
562 and Tungsten. Elsevier, pp. 749–769. https://doi.org/10.1016/b978-0-08-018868-
563 3.50012-4

564 Satheeshkumar, M.K., Ranjith Kumar, E., Srinivas, C., Prasad, G., Meena, S.S., Pradeep, I.,
565 Suriyanarayanan, N., Sastry, D.L., 2019. Structural and magnetic properties of $CuFe_2O_4$
566 ferrite nanoparticles synthesized by cow urine assisted combustion method. J. Magn.
567 Magn. Mater. 484, 120–125. https://doi.org/10.1016/j.jmmm.2019.03.128

568 Schreck, M., Wagner, J., 2017. Incentivizing secondary raw material markets for sustainable
569 waste management. Waste Manag. 67, 354–359.
570 https://doi.org/10.1016/j.wasman.2017.05.036

571 Sherman, D.M., Ragnarsdottir, K.V., Oelkers, E.H., Collins, C.R., 2000. Speciation of tin (Sn^{2+}
572 and Sn^{4+}) in aqueous Cl solutions from 25°C to 350°C: An in situ EXAFS study, in:
573 Chemical Geology. Elsevier, pp. 169–176. https://doi.org/10.1016/S0009-
574 2541(99)00208-9

575 Shukla, G., Shahi, V.K., 2019. Sulfonated poly(ether ether ketone)/imidized graphene oxide
576 composite cation exchange membrane with improved conductivity and stability for

electrodialytic water desalination. Desalination 451, 200–208. https://doi.org/10.1016/j.desal.2018.03.018

USEPA, 2007. EPA method 3051A - Microwave Assisted Acid Digestion of Sediments, Sludges, Soils, and Oils, US Environmental Protection Agency.

Vempati, R., Mollah, Y., Chinthala, A., Cocke, D., 1995. Solidification/stabilization of toxic metal wastes using coke and coal combustion by-products. Waste Manag. 15, 433–440.

Xi, Y., Zou, J., Luo, Y., Li, J., Li, X., Liao, T., Zhang, L., Wang, C., Lin, G., 2019. Performance and mechanism of arsenic removal in waste acid by combination of $CuSO_4$ and zero-valent iron. Chem. Eng. J. 375, 121928. https://doi.org/10.1016/j.cej.2019.121928

Yang, J., Bourgeois, F., Bru, K., Hakkinen, A., Andreiadis, E., Meyer, D., Bellier, Q., BArt, H.-J., Virolainen, S., Lambert, J.-M., Leszcynska-Sejda, K., Kurylak, W., Sundqvist, L., Ye, G., Yang, Y., 2016. State of the art on the recovery of refractory metals from primary resources, MSP-REFRAM, European Union's Horizon 2020 Research & Innovation programme under Grant Agreement no. 688993, accessed March 20th, 2020, http://prometia.eu/deliverables/.

Yang, J., Chai, L., Yue, M., Li, Q., 2015. Complexation of arsenate with ferric ion in aqueous solutions. RSC Adv. 5, 103936–103942. https://doi.org/10.1039/c5ra21836e

Yekta, S., Sadeghi, M., Babanezhad, E., 2016. Synthesis of $CaWO_4$ nanoparticles and its application for the adsorption-degradation of organophosphorus cyanophos. J. Water Process Eng. 14, 19–27. https://doi.org/10.1016/j.jwpe.2016.10.004

Zhang, Z., Ottosen, L.M., Wu, T., Jensen, P.E., 2019. Electro-remediation of tailings from a multi-metal sulphide mine: comparing removal efficiencies of Pb, Zn, Cu and Cd. Chem. Ecol. 35, 54–68. https://doi.org/10.1080/02757540.2018.1529173

Graphical Abstract

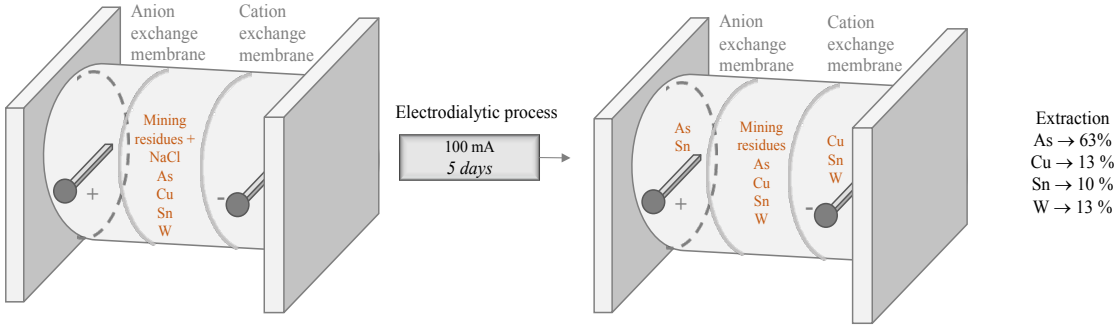

Appendix A Supplementary data

*Table S1. Initial and final pH and conductivity values in the electrolytes' compartments on regular and control ED experiments. E1-CEM, 100 mA; E2-AEM, 100 mA; E3-AEM, 50 mA; C1-control AEM; C2-control CEM; C3-control AEM-CEM; BW-AEM-CEM, NaCl, 100 mA; EF1-AEM, 50 mA; EF2-CEM, 50 mA; EF3-AEM, 65-55-45-35 mA (*sequential current intensity).

Experiment	Electrolyte	pH		Conductivity (mS/cm)	
		Initial	Final	Initial	Final
E1	Catholyte	6.1 ± 0.4	9.8 ± 1.2[a]	1.2 ± 0.1	4.5 ± 4.3
E2	Anolyte	5.2 ± 0.6	1.6 ± 0.1[A,b]	0.7 ± 0.5	6.3 ± 1.6
E3	Anolyte	5.3 ± 0.6	1.8 ± 0.4[A,c]	0.9 ± 0.1	4.1 ± 0.5
C1	Anolyte	6.1 ± 0.3	4.9 ± 0.1[A]	1.2 ± 0.4	1.1 ± 0.1
C2	Catholyte	6.1 ± 0.3	4.1 ± 0.6[A,d]	1.2 ± 0.4	1.0 ± 0.1
C3	Anolyte	5.7 ± 0.9	1.9 ± 0.1[A,e]	1.4 ± 0.1	3.1 ± 0.6
	Catholyte		8.2 ± 1.8[B,C,D,E]		1.3 ± 0.1

Statistical analysis was carried out at $p < 0.05$ (95% confidence interval). Data with lower case letters are statistically significantly different to data with the same capital letter.

609 *Table S2. Effluent initial characterisation.*

	Total suspended solids (mg/L)	Cl^-	NO_3^-	SO_4^{2-}
Effluent*	< 15	193	82	28

610 *Data from (Magro et al., 2020)